

Energetics and Structures of the Carbonyl Chloride Radical, Oxalyl Chloride, and Their Cations

Siu-Hung Chien, Kai-Chung Lau, and Wai-Kee Li*

Department of Chemistry, The Chinese University of Hong Kong, Shatin, N.T., Hong Kong

C. Y. Ng*

Ames Laboratory,[†] USDOE, and Department of Chemistry, Iowa State University, Ames, Iowa 50011

Received: June 24, 1999

An ab initio study on the structures and energetics of the carbonyl chloride radical and its dimer, oxalyl chloride, along with their cations, was carried out using the Gaussian-2 (G2) and Gaussian-3 (G3) models of theory. The structural results obtained include optimized geometries of CICO, CICO⁺, the anti, syn, and gauche conformers of (CICO)₂ and the transition structure (TS) connecting the anti and gauche conformers, and (CICO)₂⁺. The energetic results reported include the heats of formation for CICO, various (CICO)₂ conformers and transition structures, CICO⁺, and (CICO)₂⁺, as well as the adiabatic and vertical ionization energies of CICO and (CICO)₂. The G3 results obtained are in very good agreement with the available experimental data. In some cases, where the experimental data are unavailable or imprecise, the G3 results should be reliable estimates. Among the three experimental ΔH_{f298}° values for CICO found in the literature, the one most recently reported (-21.8 ± 2.5 kJ mol⁻¹) has the best agreement with the G3 result (-19.4 kJ mol⁻¹). For oxalyl chloride, we located a gauche conformer and a TS linking the anti and gauche conformers at the MP2(Full)/6-311+G(3df,2p) level, in qualitative agreement with the experimental findings. Also, both experimental and computational results agree that both the anti and gauche conformers lie in very flat potential minima. Based on the limited number of systems studied in this work, the G3 model yields results which are in better agreement with the experimental data than the G2 method.

Introduction

The carbonyl chloride free radical, CICO, was first postulated to be an intermediate in the reaction of Cl₂ with CO to form phosgene about 70 years ago.^{1,2} However, the CICO radical was not directly observed until 1965. When Cl atoms were produced by the photolysis of HCl, Cl₂, Cl₂CO, and (CICO)₂ (oxalyl chloride) in a matrix at 14 K, the Cl atoms reacted with CO to form CICO, with no activation energy required.³ In the same experiment, the infrared spectrum of CICO was also recorded. More recently, in a photodissociation dynamics study of oxalyl chloride, the upper bound of the ionization energy (IE) of CICO was estimated to be 11.5 ± 0.3 eV. Also, since the Franck–Condon factors are not known, the true IE “could be somewhat lower.”⁴ In addition, there is a significant discrepancy between the heats of formation at 298 K (ΔH_{f298}°) for this radical reported in the literature: -16.7 ± 12.6 kJ mol⁻¹⁵ and -62.8 ± 42 kJ mol⁻¹.⁶ More recently, Wine and co-workers⁷ have measured the ΔH_{f0}° and ΔH_{f298}° values for CICO to be -23.4 ± 2.9 and -21.8 ± 2.5 kJ mol⁻¹, respectively. In this work, among other things, we wish to resolve the difference among the measured experimental data.

The dimer of the CICO radical, oxalyl chloride, is an interesting molecule by its own right. For the past 45 years, there have been numerous studies on the internal rotation around

the C–C bond. Experimentally, in addition to the anti conformer (with the dihedral angle ClCCl equal to 180°), there appears to be a gauche conformer with this dihedral angle being about 80°. On the other hand, a number of theoretical attempts to locate this gauche conformer failed. In 1995, Hedberg and co-workers⁹ finally located this conformer at the MP2(Full)/TZ2P level. At this level of theory, the gauche conformer has a ClCCl dihedral angle of 89.8° and the gauche-anti barrier is only about 0.13 kJ mol⁻¹. Hence, while theory and experiment agree qualitatively on the existence of the gauche conformer, the theoretical evidence for this existence is very tenuous indeed. Here, we performed calculations at higher levels with the hope of establishing the existence of the gauche conformer on a firmer basis.

To sum up, in this work, we carried out an ab initio structural and energetic studies on carbonyl chloride and oxalyl chloride, as well as their cations. The computational models we employed were the Gaussian-2 (G2)¹⁰ and the more recently developed Gaussian-3 (G3)¹¹ methods. In this paper, we report the optimized structures and the ΔH_f° values for all these species, along with the adiabatic and vertical IEs for CICO and anti (CICO)₂. Where applicable, we compare these results with experimental data. In addition, we will also use the calculated results to assess the relative merits of the G2 and G3 models.

Computational Methods and Results

All calculations were carried out on DEC 500au, IBM RS6000/390, and SGI 10000 workstations, and SGI Origin 2000 High Performance Server, using the Gaussian 94 package of

* Authors to whom correspondence should be addressed.

[†] Ames Laboratory is operated for the U.S. Department of Energy by Iowa State University under Contract W-7405-Eng-82. This article was supported by the Division of Chemical Sciences, Office of Basic Energy Sciences.

the programs.¹² All structures were optimized at the second-order Møller–Plesset theory (MP2) using the 6-31G(d) basis set with all electrons included, i.e., at the MP2(Full)/6-31G(d) level. The G2 theoretical procedure is an approximation to the ab initio level of QCISD(T)/6-311+G(3df,2p). It requires single-point energy calculations at the QCISD(T)/6-311G(d,p), MP4/6-311G(d,p), MP4/6-311+G(d,p), MP4/6-311G(2df,p), and MP2/6-311+G(3df,2p) levels based on the optimized geometry at MP2(Full)/6-31G(d). A small empirical correction is added to include higher level correction (HLC) effects in the calculation of the total electronic energies (E_e). The MP2(Full)/6-31G(d) harmonic vibrational frequencies, scaled by 0.9646, are applied for the zero-point vibrational energy (ZPVE) correction at 0 K ($E_0 = E_e + \text{ZPVE}$).

In the G3 model, geometry optimization and ZPVE correction are also done at the MP2(Full)/6-31G(d) level. On the other hand, the G3 model requires single-point calculations at QCISD(T)/6-31G(d), MP4/6-31G(d), MP4/6-31+G(d), MP4/6-31G(2df,p), and MP2(Full)/G3large levels, where G3large is a triple- ζ basis proposed by Curtiss et al.¹¹ In addition, this model also includes HLC as well as spin-orbit coupling correction (the latter only for monatomic species). The average absolute deviation from experiment for the 148 calculated G3 enthalpies of formation is 3.9 kJ mol⁻¹, compared to the G2 average absolute deviation of 6.5 kJ mol⁻¹.¹¹

As mentioned earlier, the gauche conformer of oxalyl chloride and the transition structure (TS) linking the gauche and anti conformers of this compound could not be located at many levels of theory,⁹ including MP2(Full)/6-31G(d). In this work, we optimized the geometries of these three structures (anti, TS, and gauche) at the MP2(Full)/6-311+G(3df,2p) level. Additionally, we characterized these stationary points as minimum and first-order saddle point by vibrational frequency calculations. Then we carried out G2 and G3 calculations with geometries optimized at this level. Also, for the temperature dependence and ZPVE corrections, we used the vibrational frequencies calculated at the MP2(Full)/6-311+G(3df,2p) level, scaled by a factor of 0.97.¹³

For all the species studied in this work, the G2 and G3 heats of formation were determined in the following manner.¹⁴ For molecule AB, its G2/G3 heat of formation at T ($\Delta H_{\text{f},T}^0$) was calculated from the G2/G3 heat of reaction $\Delta H_{\text{r},T}^0(\text{A} + \text{B} \rightarrow \text{AB})$ and the respective experimental $\Delta H_{\text{f},T}^0(\text{A})$ and $\Delta H_{\text{f},T}^0(\text{B})$ for elements A and B.

Before proceeding to presenting and discussing the results, we note that the G2 predictions for ΔH_{f}^0 and IE values are usually well within ± 0.10 eV (or about ± 10 kJ mol⁻¹) of the experimental data¹⁰ for relatively small systems. So far we have applied the G2 method to a number of systems¹⁴ and the results are in good to excellent agreements with the available experimental data. As the G3 method has been proposed relatively recently, so far we have applied it only to hydrochlorofluoromethanes and the results show an improvement over their G2 counterparts.¹⁵

The optimized structures of ClCO, ClCO⁺, various conformers of (ClCO)₂, and (ClCO)₂⁺ are shown in Figure 1. The G2 and G3 energies (E_0), enthalpies (H_{298}), $\Delta H_{\text{f},0}^0$, and $\Delta H_{\text{f},298}^0$ values for ClCO, ClCO⁺, anti and syn (ClCO)₂, and (ClCO)₂⁺, as well as the adiabatic and vertical IEs (IE_a and IE_v) of ClCO and anti (ClCO)₂, all based on the MP2(Full)/6-31G(d) geometries, are listed in Table 1. Tabulated in Table 2 are the G2 and G3 E_0 , H_{298} , $\Delta H_{\text{f},0}^0$, and $\Delta H_{\text{f},298}^0$ values for anti and gauche (ClCO)₂ and the TS linking them, all based on the structures optimized at the MP2(Full)/6-311+G(3df,2p) level. As the part

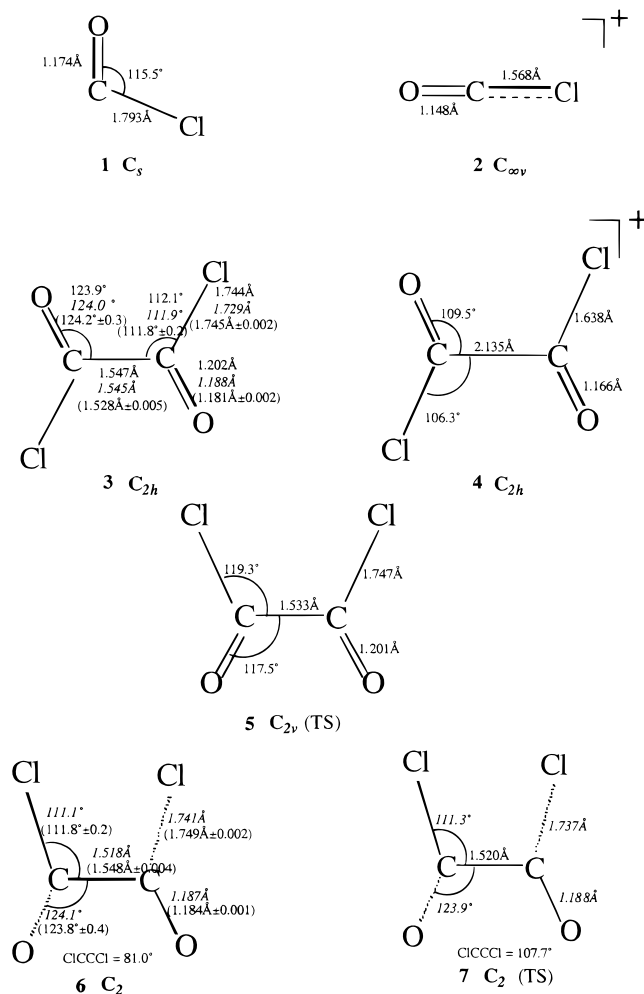


Figure 1. The structures of ClCO (1), ClCO⁺ (2), anti (ClCO)₂ (3), (ClCO)₂⁺ (4), syn (ClCO)₂ (5), gauche (ClCO)₂ (6), and the transition structure (7) linking 3 and 6. Unless stated otherwise, structures are optimized at the MP2(Full)/6-31G(d) level. The structural parameters which are optimized at the MP2(Full)/6-311+G(3df,2p) level are given in italic font, and the available experimental data (from ref 9) are given in brackets.

of potential energy surface containing the anti and gauche (ClCO)₂ and the TS linking them is very flat, we also calculated the relative energies among these three structures at a number of levels of theory. These results are summarized in Table 3. Finally, as the MP2(Full)/6-31G(d) vibrational frequencies for ClCO do not agree well with the experimental data, we also optimized this species' structure and calculated its frequencies at various additional levels. The results are given in Table 4.

Discussion

Carbonyl Chloride and Its Cation. Examining the structures of ClCO and ClCO⁺ displayed in Figure 1, the geometrical features are what would be expected from elementary bonding theory such as the valence-shell-electron-pair-repulsion model.¹⁶ Specifically, for ClCO, the carbon–chlorine and carbon–oxygen bonds are single and double bonds, respectively, while the lone electron on carbon is responsible for the bent geometry. In a more advanced language, a linear ClCO will undergo Renner–Teller distortion¹⁷ to become bent. For ClCO⁺, isoelectronic to CO₂, both bonds may be considered as double bonds and there is no nonbonding electron on carbon, leading to a linear geometry. These general descriptions are supported by the following quantitative results. At the G2 and G3 levels,

TABLE 1: G3 and G2 Total Energies^a (E_0), Enthalpies (H_{298}), and Standard Heats of Formation at 0 and 298 K (ΔH_{F0}^0 and ΔH_{F298}^0) for CICO/CICO⁺ and (CICO)₂/(CICO)₂⁺, as Well as the Adiabatic and Vertical Ionization Energies (IE_a and IE_v) of CICO and Anti (CICO)₂^b

species (symmetry)		E_0 (hartree)	H_{298} (hartree)	ΔH_{F0}^0 (kJ mol ⁻¹)	ΔH_{F298}^0 (kJ mol ⁻¹)	IE _a (eV)	IE _v (eV)
CICO (C _s)	(1)	-573.26833 <i>-572.86379</i>	-573.26407 <i>-572.85920</i>	-21.6 <i>-27.2</i> (-23.4 ± 2.9) ^e	-19.4 <i>-24.1</i> (-17 ± 13) ^c (-63 ± 42) ^d (-21.8 ± 2.5) ^e	8.28 <i>8.27</i> (<11.5 ± 0.3) ^f	10.01 <i>9.94</i>
CICO ⁺ (C _{∞v})	(2)	-572.96401 <i>-572.55972</i>	-572.95960 <i>-572.55579</i>	777.4 <i>771.1</i>	780.0 <i>772.4</i>		
anti (CICO) ₂ (C _{2h})	(3)	-1146.64722 <i>-1145.83794</i>	-1146.64036 <i>-1145.83107</i>	-333.5 <i>-344.2</i>	-333.4 <i>-344.1</i> (-335.8 ± 6.3) ^g	10.82 <i>10.81</i> (10.91 ± 0.05) ^h	11.26 <i>11.30</i> (11.33) ⁱ (11.26) ^j
(CICO) ₂ ⁺ (C _{2h})	(4)	-1146.24970 <i>-1145.44080</i>	-1146.24206 <i>-1145.43370</i>	710.2 <i>698.5</i>	712.3 <i>700.9</i>		
syn (CICO) ₂ (C _{2v})	(5)	-1146.64360 <i>-1145.83421</i>	-1146.63761 <i>-1145.82823</i>	-324.0 <i>-334.4</i>	-326.2 <i>-336.6</i>		

^a Calculated using geometries optimized at the MP2(Full)/6-31G(d) level; G3 energies are shown in bold font, and G2 energies are in italic font. ^b Experimental values, where available, are given in brackets. ^c Ref 5. ^d Ref 6. ^e Ref 7. ^f Ref 4; note that this is an *upper bound* value. ^g Ref 19. ^h Ref 20. ⁱ Ref 21. ^j Ref 22.

TABLE 2: G3 and G2 Total Energies^a (E_0), Enthalpies (H_{298}), and Standard Heats of Formation at 0 and 298 K (ΔH_{F0}^0 and ΔH_{F298}^0) for the Two Different Conformers of (CICO)₂ and the Transition Structure Linking Them

species (symmetry)		E_0 (hartree)	H_{298} (hartree)	ΔH_{F0}^0 (kJ mol ⁻¹)	ΔH_{F298}^0 (kJ mol ⁻¹)
anti (CICO) ₂ (C _{2h})	(3)	-1146.64777 <i>-1145.83893</i>	-1146.64089 <i>-1145.83205</i>	-334.9 <i>-346.8</i>	-334.8 <i>-346.7</i> (-335.8 ± 6.3) ^b
gauche (CICO) ₂ (C ₂)	(6)	-1145.64702 <i>-1145.83879</i>	-1145.63996 <i>-1145.83168</i>	-332.9 <i>-346.4</i>	-332.4 <i>-345.7</i>
TS (CICO) ₂ (C ₂)	(7)	-1146.64701 <i>-1145.83879</i>	-1146.64085 <i>-1145.83258</i>	-333.1 <i>-346.4</i>	-333.1 <i>-348.1</i>

^a Calculated using geometries optimized at the MP2(Full)/6-311+G(3df,2p) level; G3 energies are shown in bold font, and G2 energies are in italic font. ^b Experimental value, taken from ref 19, is given in brackets.

dissociation energy $D_0(\text{Cl}-\text{CO})$ is calculated to be 25.1 and 26.3 kJ mol⁻¹, respectively, in very good agreement with the experimental value of 27 kJ mol⁻¹.⁴ For CICO⁺, at the G2 and G3 levels, dissociation energy $D_0(\text{Cl}^+=\text{CO})$ is 466.0 and 471.0 kJ mol⁻¹, respectively. These values are comparable to the G2 and G3 results of $D_0(\text{O}=\text{CO})$, 529.7 and 530.2 kJ mol⁻¹, respectively.

At the HF/6-31G(d) level, the vibrational frequencies of CICO are calculated to be 197, 577, and 2167 cm⁻¹. On the other hand, at the MP2(Full)/6-31G(d) level, they are 383, 647, and 2000 cm⁻¹. These results are not in good agreement with the experimentally measured frequencies of 281, 570, and 1880 cm⁻¹.³ As this is a relatively small species, we carried out the geometry optimization and frequency calculations for CICO at a number of levels higher than MP2(Full)/6-31G(d), including B3LYP/6-31G(d), B3LYP/6-311+G(3df,2p), QCISD(T)/6-31G(d), and BD(T)/6-31G(d). Examining the results summarized in Table 4, it is seen that the results of the two last-mentioned levels agree fairly well with the experimental data, even though ν_1 still does not come out well at either of these levels. It appears that correlation at a very high level is required for the accurate frequency calculations of this species.

The G2 and G3 ΔH_{F298}^0 for CICO are calculated to be -24.1 and -19.4 kJ mol⁻¹. The G3 result is in excellent accord with the experimental data of -21.8 ± 2.5 kJ mol⁻¹, reported by Wine and co-workers.⁷ In addition, the G3 ΔH_{F0}^0 (-21.6 kJ mol⁻¹) for this radical is also in good agreement with that reported by the same researchers, -23.4 ± 2.9 kJ mol⁻¹. In other words, among the three rather dissimilar experimental

values of ΔH_{F298}^0 for CICO, both G2 and G3 results favor that measured by Wine et al.,⁷ which is also the most recently reported data.

As shown in Table 1, the G2 IE_a and IE_v of CICO are calculated to be 8.27 and 9.94 eV, respectively, while those for G3 are 8.28 and 10.01 eV. Both sets of values are well below the experimental *upper bound* reported by Hemmi and Suits,⁴ 11.5 ± 0.3 eV. This is not unexpected, since CICO and CICO⁺ have significantly different structures, as shown in Figure 1 and discussed above.

The Anti and Syn Conformers of Oxalyl Chloride and Oxalyl Chloride Cation. As shown in Figure 1, the optimized structures of the anti conformer of oxalyl chloride (**3**) are in very good agreement with the available experimental findings.^{9,18} Also, the two levels of theory used in geometry optimization, MP2(Full)/6-31G(d) and MP2(Full)/6-311+G(3df,2p), lead to very similar results. As expected, the syn conformer (**5**) represents a TS on the energy surface and its structural features are similar to those of **3**, aside from the dihedral angles defining the conformation. Referring to the structure of (CICO)₂⁺ (**4**) shown in Figure 1, it is seen that, upon ionization, the C-C bond has lengthened considerably. This is consistent with that the highest occupied molecular orbital (with A_g symmetry) has significant bonding interaction between the orbitals on the two carbon atoms.

Referring to Table 1, where all energies are calculated on the basis geometries optimized at the MP2(Full)/6-31G(d) level, the G3 and G2 ΔH_{F298}^0 of **3** are calculated to be -333.4 and -344.1 kJ mol⁻¹, respectively. The former is once again in

TABLE 3: Total Energies^a (in hartree) and Relative Energies (ΔE^b , in kJ mol⁻¹) for the Two Conformers of (CICO)₂ and the Transition Structure Linking Them at Different Levels of Theory

	anti (CICO) ₂ (3)	TS (CICO) ₂ (7)	gauche (CICO) ₂ (6)
MP2(Full)/6-311+G(3df,2p)	-1145.97283	-1145.97185	-1145.97203
ZPVE	0.01992	0.01975	0.01978
ΔE	0.0 (0.0)	2.6 (2.1)	2.1 (1.7)
MP4/6-31G(d)	-1145.33788	-1145.33570	-1145.33512
ΔE	0.0 (0.0)	5.7 (5.3)	7.2 (6.9)
QCISD(T)/6-31G(d)	-1145.33025	-1145.32774	-1145.32707
ΔE	0.0 (0.0)	6.6 (6.1)	8.3 (8.0)
MP4/6-31+G(d)	-1145.35745	-1145.35785	-1145.35722
ΔE	0.0 (0.0)	-1.1 (-1.5)	0.6 (0.2)
MP4/6-311G(d,p)	-1145.50751	-1145.50605	-1145.50577
ΔE	0.0 (0.0)	3.8 (3.4)	4.6 (4.2)
MP4/6-311+G(d,p)	-1145.52613	-1145.52655	-1145.52611
ΔE	0.0 (0.0)	-1.1 (-1.5)	0.1 (-0.3)
MP4/6-31G(2df,p)	-1145.60175	-1145.59934	-1145.59919
ΔE	0.0 (0.0)	6.3 (5.9)	6.7 (6.4)
QCISD(T)/6-311G(d)	-1145.49826	-1145.49650	-1145.49612
ΔE	0.0 (0.0)	4.6 (4.2)	5.6 (5.3)
MP4/6-311G(2df,p)	-1145.74793	-1145.74648	-1145.74651
ΔE	0.0 (0.0)	3.8 (3.4)	3.7 (3.4)
G2 ^c	-1145.83893	-1145.83879	-1145.83879
ΔE	0.0	0.4	0.4
G3 ^c	-1146.64777	-1146.64701	-1146.64702
ΔE	0.0	2.0	2.0
MP4/6-311+G(3df,2p)	-1145.78361	-1145.78328	-1145.78344
ΔE	0.0 (0.0)	0.9 (0.4)	0.4 (0.1)
QCISD(T)/6-311+G(3df,2p)	-1145.77160	-1145.77083	-1145.77086
ΔE	0.0 (0.0)	2.0 (1.6)	1.9 (1.6)
MP4/G3large	-1146.47394	-1146.47278	-1146.47292
ΔE	0.0 (0.0)	3.0 (2.6)	2.7 (2.3)

^a Calculated using geometries optimized at the MP2(Full)/6-311+G(3df,2p) level. ^b Relative energy including ZPVE (scaled by 0.97) correction are given in brackets. ^c The ZPVE corrections are calculated using MP2(Full)/6-311+G(3df,2p) frequencies, scaled by 0.97.

TABLE 4: Calculated Structural Parameters and Vibrational Frequencies of CICO at Different Levels of Theory

Level	C–O (Å)	C–Cl (Å)	O–C–Cl (°)	ν_1 (A') (cm ⁻¹)	ν_2 (A') (cm ⁻¹)	ν_3 (A') (cm ⁻¹)
HF/6-31G(d)	1.135	1.840	115.5	197	577	2167
MP2(Full)/6-31G(d)	1.174	1.793	115.5	383	647	2000
B3LYP/6-31G(d)	1.164	1.840	115.6	332	589	1966
B3LYP/6-311+G(3df,2p)	1.155	1.805	115.2	358	595	1943
QCISD(T)/6-31G(d)	1.175	1.828	115.7	328	585	1902
BD(T)/6-31G(d)	1.176	1.809	115.6	350	590	1990
experimental ^a	1.170	1.750	120.0	281	570	1880

^a Experimental values are taken from ref 3.

excellent agreement with the reported experimental value of -335.8 ± 6.3 kJ mol⁻¹.¹⁹ Also, both the calculated adiabatic and vertical IEs of **3** are in very good agreement with the available experimental data in the literature. Finally, it is noted that **5** is less stable than **3** by about 7 kJ mol⁻¹, which implies there is free rotation about the C–C bond of **3** at room temperatures.

The Anti and Gauche Conformers of (CICO)₂ and the TS Linking Them. As mentioned previously, the gauche conformer (**6**) of (CICO)₂ cannot be located at either HF or MP2(Full) levels using the 6-31G(d) basis. On the hand, Hedberg et al. did find **6** at the MP2(Full)/TZ2P level.⁹ In this work, we also located **6** at the level of MP2(Full)/6-311+G(3df,2p). In other words, **6** is not artifact of one level of theory. However, it cannot be located unless a fairly large basis set is used. There are only slight differences between the structures of **6** optimized at the two aforementioned levels. In particular, we note that, at the MP2(Full)/TZ2P level, the ClCCl dihedral angle has a value of 89.8°;⁹ at the MP2(Full)/6-311+G(3df,2p) level, this torsion angle becomes 81.0°, in good agreement with the experimental result, 76 ± 9 °.⁹ On the other hand, for the TS (**7**) linking **3** and **6**, the ClCCl dihedral angle is 107.7°. This value is fairly

close to that in **6**, indicating a very low barrier for the transformation (see below).

Referring to Table 2, where the energies are calculated using the geometries optimized at the MP2(Full)/6-311+G(3df,2p) level, it is seen that the G3 ΔH°_{298} value of **3** shows an improvement of 1.4 kJ mol⁻¹ over that calculated using the MP2(Full)/6-31G(d) geometry (listed in Table 1). At the G3 level, **3** is more stable than **6** by 2.0–2.4 kJ mol⁻¹. At the G2 level, this energy gap becomes 0.4–1.0 kJ mol⁻¹. More disturbingly, the TS **7** linking **3** and **6** becomes slightly more stable than **6**. This type of situation occurs often when an extremely flat surface is investigated using different levels of theory for geometry optimization and energy comparison. As we recall, in this case, geometry optimization is done at the MP2(Full)/6-311+G(3df,2p) level, while energies are calculated employing additivity relations among single-point energies calculated with smaller basis sets. We are going to discuss this point in a more detailed manner in the next paragraph.

Let us now refer to Table 3, where we compare the relative energies of **3**, **6**, and **7** at a variety levels of theory, using the MP2(Full)/6-311G(3df,2p) geometries. It is seen that **3** remains the most stable species at most of the levels studied. The

exceptions are MP4/6-31+G(d) and MP4/6-311+G(d,p), where the most stable species is **7**, the TS linking **3** and **6**. Also, at all levels employing basis set smaller than 6-311+G(3df,2p), including G2 and G3 models, we do not get the expected energy ordering of **3** < **6** < **7**. This is because these structures have energies within about 2–3 kJ mol⁻¹ of each other, and we need a very large basis set to gauge such a small difference. On the other hand, with this large basis, correlation level MP2(Full) or MP4 or QCISD(T) can lead to the right ordering. In any event, based on the results summarized in Table 3, among these three structures, **3** is more stable than **6** by about 2 kJ mol⁻¹ and the TS **7** is less stable than **6** by about 1 kJ mol⁻¹.

Conclusions

We carried out an ab initio structural and energetics study at the G2 and G3 levels of theory on carbonyl chloride and its dimer, oxalyl chloride, as well as their cations. On the basis of the results obtained, the following conclusions may be drawn.

(1) The G2 and G3 results obtained are in very good agreement with the available experimental data. In some cases, when the experimental data are unavailable in the literature or imprecise, the G3 results should give reliable estimates.

(2) Among the three experimental ΔH_{1298}° values for ClCO reported in the literature, the one measured by Wine and co-workers⁷ (-21.8 ± 2.5 kJ mol⁻¹) has the best agreement with the G3 result (-19.4 kJ mol⁻¹).

(3) For oxalyl chloride, we located a gauche conformer and a TS linking the anti and gauche conformers at the MP2(Full)/6-311+G(3df,2p) level, in qualitative agreement with the experimental findings. This result shows that the gauche conformer found by Hedberg et al.⁹ is not an artifact of the computational level they employed. Also, both experimental and computational results agree that both the anti and gauche conformers lie in very flat potential minima.

(4) Based on the admittedly limited number of systems studied in this work, the G3 model yields results which are in better agreement with the experimental data than the G2 method. This is particularly helpful since the G3 calculations require less computational resources than the G2.

Acknowledgment. The authors from The Chinese University of Hong Kong are grateful to their Computer Services Centre for generous time allocation on the SGI Origin 2000 High Performance Server. C.Y.N. acknowledges the support of the

Alexander von Humboldt Senior Scientist Award and the U.S. Department of Energy under Contract No. W-7405-Eng-82 for the Ames Laboratory.

References and Notes

- (1) Bodenstein, M.; Lenher, S.; Wagner, C. *Z. Physik. Chem.* **1929**, *B3*, 459.
- (2) Lenher, S.; Rollefson, G. K. *J. Am. Chem. Soc.* **1930**, *52*, 500.
- (3) Jacox, M. E.; Milligan, D. E. *J. Chem. Phys.* **1965**, *43*, 866.
- (4) Hemmi, N.; Suits, A. G. *J. Phys. Chem. A* **1997**, *101*, 6633.
- (5) Walker, L. C.; Prophet, H. *Trans. Faraday Soc.* **1967**, *63*, 879.
- (6) Chase, M. W.; Davies, C. A.; Downey, J. R.; Frurip, O. J.; McDonald, R. A.; Syverud, A. N. *J. Phys. Chem. Ref. Data* **1985**, *14*, Suppl. 1.
- (7) Nicovich, J. M.; Kreutter, K. D.; Wine, P. H. *J. Chem. Phys.* **1990**, *92*, 3539.
- (8) Danielson, D. D. Ph.D. Thesis, Oregon State University, 1980.
- (9) Danielson, D. D.; Hedberg, L.; Hedberg K.; Hagen, K.; Tratteberg, M. *J. Phys. Chem.* **1995**, *99*, 9374.
- (10) Curtiss, L. A.; Raghavachari, K.; Trucks, G. W.; Pople, J. A. *J. Chem. Phys.* **1991**, *94*, 7221.
- (11) Curtiss, L. A.; Raghavachari, K.; Redfern, P. C.; Redfern V.; Pople, J. A. *J. Chem. Phys.* **1998**, *109*, 7764.
- (12) Frisch, M. J.; Trucks, G. W.; Schlegel, H. B.; Gill, P. M. W.; Johnson, B. J.; Robb, M. A.; Cheeseman, J. R.; Keith, T. A.; Petersson, G. A.; Montgomery, J. A.; Raghavachari, K.; Al-Laham, M. A.; Zarkewski, V. G.; Ortiz, J. V.; Foresman, J. B.; Cioslowski, J.; Stefanov, B. B.; Nanayakkara, A.; Challacombe, M.; Peng, C. Y.; Anala, P. Y.; Chen, W.; Wong, M. W.; Andres, J. L.; Replogle, E. S.; Gomperts, R.; Martin, R. L.; Fox, D. J.; Binkley, J. S.; Defrees, D. J.; Baker, J.; Stewart, J. J. P.; Head-Gordon, M.; Gonzalez, C.; Pople, J. A. *GAUSSIAN 94*, Revision D4; Gaussian, Inc.: Pittsburgh, PA, 1995.
- (13) To come up with this scaling factor, we have taken into account the various scaling factors evaluated at different levels of theory: Scott, A. P.; Radom, L. *J. Phys. Chem.* **1996**, *100*, 16502.
- (14) Chiu, S.-W.; Cheung, Y.-S.; Ma, N. L.; Li, W.-K.; Ng, C. Y. *J. Mol. Struct. (THEOCHEM)* **1998**, *452*, 97; Chiu, S.-W.; Cheung, Y.-S.; Ma, N. L.; Li, W.-K.; Ng, C. Y. *J. Mol. Struct. (THEOCHEM)* **1999**, *468*, 21; Li, W.-K.; Ng, C. Y. *J. Phys. Chem. A* **1997**, *101*, 113.
- (15) Ma, N. L.; Lau, K.-C.; Chien, S.-H.; Li, W.-K. *Chem. Phys. Lett.*, in press.
- (16) Gillespie, R. J.; Hargittai, I. *The VSEPR Model of Molecular Geometry*; Allyn and Bacon: Boston, 1991.
- (17) Renner, R. Z. *Physik. Chem.* **1934**, *92*, 172.
- (18) Hagen, K.; Hedberg, K. *J. Am. Chem. Soc.* **1973**, *95*, 1003.
- (19) Pedley, J. B.; Naylor, R. D.; Kirby, S. *Thermodynamical Data of Organic Compounds*; Chapman and Hall: New York, 1986.
- (20) Frost, D. C.; McDowell, C. A.; Pouzard, G.; Westood, N. P. C. *J. Electron Spectrosc. Relat. Phenom.* **1977**, *10*, 273.
- (21) Kimura, K.; Katsumata, S.; Achiba, Y.; Yamazaki, T.; Iwata, S. *Handbook of HeI Photoelectron Spectra of Fundamental Organic Compounds*; Japan Scientific Soc. Press: Tokyo, 1981.
- (22) Meeks, J. L.; McGlynn, S. P. *Spectrosc. Lett.* **1975**, *8*, 439.
- (23) Curtiss, L. A.; Raghavachari, K.; Pople, J. A. *J. Chem. Phys.* **1993**, *98*, 12.